Paper

Fabrication of a Common-mode Noise Filter for Balanced-mode Signal Transmission using Mn-Zn Ferrite Particle/Polyimide Composite Thick Film

Toshiro Sato* Member
Takahiro Kokai* Non-member
Masashi Moroishi* Non-member
Kiyohito Yamasawa* Member
Toshiyuki Sakuma** Non-member
Hiroki Karasawa** Non-member
Koichi Hirasawa** Member

To develop a common-mode noise filter for balanced-mode digital signal interfaces such as USB ver.2 and IEEE 1394, a Mn-Zn ferrite/Polyimide composite thick film was fabricated and applied to the filter device. The polycrystalline Mn-Zn ferrite powder and polyimide precursor liquid solution were used as the starting materials for the composite thick film. The composite film had a large imaginary part of complex permeability at high frequencies over 1GHz, and high permittivity. The common-mode noise filter using the composite film exhibited the common-mode suppression of over 10dB in the frequency range over 1GHz.

Keywords: common-mode filter, composite thick film, Mn-Zn ferrite powder, polyimide, USB, IEEE1394

1. Introduction

The balanced-mode digital signal interfaces such as USB and IEEE 1394 [1] [2] have been used for the signal interconnection between various digital instruments such as personal computer, digital camera, digital VCR and so on. Since such signal interfaces have a balanced signal transmission-line consisting of a pair of twisted conductor lines, the electromagnetic interference for the ambient electronic apparatus becomes small enough. However, when the signal source has an unbalanced component, the electromagnetic radiation due to the unbalanced common-mode current becomes large.

Tsuda et al. developed a coupled transmission-line common-mode filter [3], which consisted of an alumina dielectric material with a relative permittivity of about 10, and a pair of the inner molybdenum spiral windings. For the common-mode signal, the device exhibited a band stop filter characteristic with a center frequency of 900 MHz and a bandwidth of 500 MHz. The narrow bandwidth for the common-mode suppression was due to the very small dielectric loss of the alumina material. Insertion loss for the balanced mode signal was 3～8 dB. The large insertion loss for the balanced mode signal was due to the weak magnetic coupling between two spiral windings. The weak magnetic coupling was owing to the nonmagnetic alumina material with a relative permeability of unity.

The authors also reported a coupled transmission-line common-mode filter using Ni-Zn ferrite substrate [4]. Since the Ni-Zn ferrite used in the device had a relative permeability of 10 and a relative permittivity of 10, the electromagnetic coupling between the conductor lines was expected to be stronger than that of the device using nonmagnetic dielectric material. In addition, since the magnetic loss of the ferrite was large at high frequencies around or over 1 GHz, the wideband common-mode noise absorption was also expected. However, since the previous device was fabricated by the adhesion technique using the polyimide precursor liquid solution, the device exhibited the deviated characteristic from the designed one. This was owing to the undesired thicker polyimide adhesion layer.

Recently, the authors have fabricated a composite film with polycrystalline Mn-Zn ferrite particle and polyimide [5]. The composite film exhibited a large imaginary part of complex permeability at high frequencies over 1GHz. In addition, the film also had a high relative permittivity of several tens.

This paper describes a common-mode noise filter using the Mn-Zn ferrite particle/polyimide composite thick film. By using the composite thick film, it was easy to fabricate the common mode noise filter without using the adhesion process. The filter configuration, basic properties of the composite material, and filter characteristics are shown in the next sections.

2. Common-Mode Noise Filter

2.1 Filter Configuration Fig. 1 shows a configuration of a common-mode noise filter using the composite thick film. The device had a pair of aluminum conductor lines embedded in the composite thick film, an upper silver paste ground plane, and a bottom aluminum substrate ground plane. As mentioned later, the electrical conductivity of the composite material was relatively high. Therefore, to decrease the leak current between the conductor line and ground plane, the inner aluminum lines were coated with polyimide insulating thin layer.

2.2 Operation Principle Since the common-mode filter

* Faculty of Engineering, Shinshu University
4-17-1, Wakazato, Nagano 380-8553
** KOA Corporation
Minowa-cho, Kami-Ina-gun, Nagano 399-4697

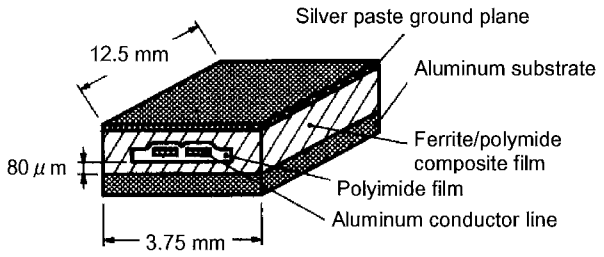

Fig. 1. Common-mode noise filter using composite thick film with Mn-Zn ferrite particle and polyimide

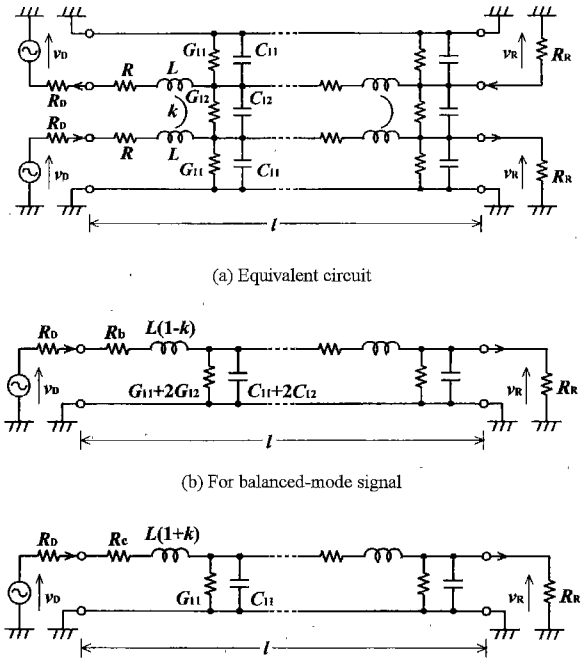

Fig. 2. Equivalent circuit of common-mode noise filter

consists of the inner coupled aluminum lines between the top and bottom ground planes, it functions as a coupled distributed constant circuit. The detailed operation principle of the filter is nearly the same as the previous device [4].

The equivalent circuit of the device is shown in Fig. 2, which is shown as the coupled distributed constant circuit. In the figure, L is the distributed line inductance, which is enhanced by the magnetic material. The magnetic coupling coefficient between conductor lines is represented as a symbol "k". R is the distributed series resistance. The upper and lower magnetic/dielectric composite layers give rise to the distributed capacitance C_{11} and conductance G_{11}. C_{12} and G_{12} are the distributed capacitance and conductance between the inner two conductor lines. l is the length of the inner conductor lines.

The equivalent circuits for the balanced-mode signal and unbalanced common-mode signal are represented in Fig. 2(b) and (c) [4]. The characteristic impedance Z_c and propagation constants γ for both signal conditions can be written as follows;

$$Z_{cb} = \left\{ \frac{R_b + j\omega L(1-k)}{G_{11} + 2G_{12} + j\omega(C_{11} + 2C_{12})} \right\}^{1/2} \quad \cdots\cdots (1)$$

$$Z_{cc} = \left\{ \frac{R_c + j\omega L(1+k)}{G_{11} + j\omega C_{11}} \right\}^{1/2} \quad \cdots\cdots (2)$$

$$\gamma_b = \left[\{R_b + j\omega L(1-k)\} \{G_{11} + 2G_{12} + j\omega(C_{11} + 2C_{12})\} \right]^{1/2} = \alpha_b + j\beta_b \quad \cdots\cdots (3)$$

$$\gamma_c = \left[\{R_c + j\omega L(1+k)\} \{G_{11} + j\omega C_{11}\} \right]^{1/2} = \alpha_c + j\beta_c \quad \cdots\cdots (4)$$

where Z_{cb} and γ_b are the values for the balanced-mode signal, Z_{cc} and γ_c are the values for the unbalanced common-mode signal, ω is the angular frequency, respectively. As mentioned later, since $G_{11} >> G_{12}$, $C_{11} >> C_{12}$ in the fabricated device, Eqs.(1) and (3) are approximated as follows;

$$Z_{cb} \fallingdotseq \left\{ \frac{R_b + j\omega L(1-k)}{G_{11} + j\omega C_{11}} \right\}^{1/2} \quad \cdots\cdots (5)$$

$$\gamma_b \fallingdotseq \left[\{R_b + j\omega L(1-k)\} \{G_{11} + j\omega C_{11}\} \right]^{1/2} \quad \cdots\cdots (6)$$

The magnetic loss depends on the signal conditions. In case of the balanced-mode signal, magnetomotive force (*m.m.f.*) becomes small, which is due to the counter currents flowing in the inner two lines. Therefore, the magnetic loss becomes small for the balanced-mode signal. On the other hand, in case of the unbalanced common-mode signal, *m.m.f.* becomes large, which is due to the in-phase currents flowing in the inner two lines. Therefore, the magnetic loss becomes large for the unbalanced common-mode signal. Because of $R_c >> R_b$ and $0 < k < 1$, Z_{cc} becomes greater than Z_{cb}, and α_c becomes greater than α_b.

If the common-mode noise filter is used for 50Ω system of the balanced-mode signal transmission, the noise filter should have Z_{cb} of 50 Ω and small α_b for obtaining small signal-reflection and small signal-decay for the balanced-mode signal transmission. On the other hand, the device should have large α_c for the unbalanced common-mode signal.

3. Mn-Zn Ferrite/Polyimide Composite Film

3.1 Fabrication Method Polycrystalline Mn-Zn ferrite powder and polyimide precursor solution were used as the starting materials for the composite thick film. The Mn-Zn ferrite powder with a mean particle diameter of 3μm had a saturation magnetization of about 5 kG, a dc coercive force of about 49 Oe, and a dc conductivity of 0.3 S/m. The polyamic acid solution with a viscosity of 800 cp was used. The Mn-Zn ferrite powder and polyamic acid solution with both same weights were mixed, and degassed in vacuum.

The mixture slurry of the Mn-Zn ferrite powder and polyamic acid solution was spun on the substrate by using a spin coater, and cured at a temperature of 300 °C for 60 minutes. Since the polyamic acid changed into the polyimide through the curing process, the cured film became the Mn-Zn ferrite particle/ polyimide composite material.

3.2 Microstructure Fig. 3 shows a photograph of the cross-sectional SEM observation for the composite thick film with a thickness of 80μm. A number of a few μm size grains were dispersed homogeneously. Though not shown here, from result of X-ray micro analyzer, Mn-Zn ferrite particles were dispersed homogeneously without local concentration [5].

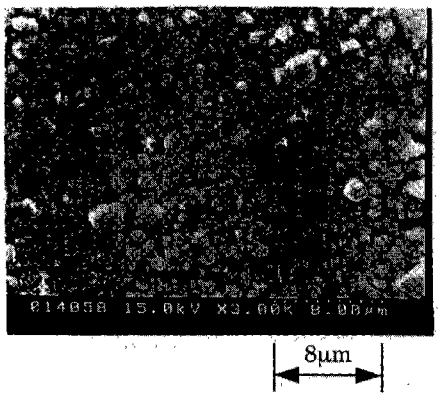

Fig. 3. Cross sectional SEM image of composite thick film

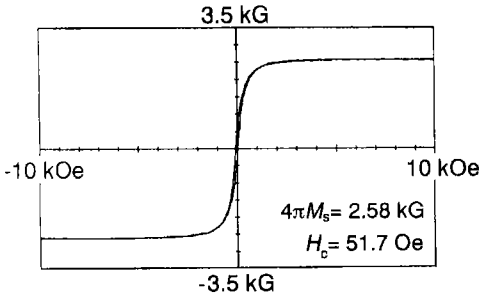

Fig. 4. Typical static magnetization curve of composite thick film

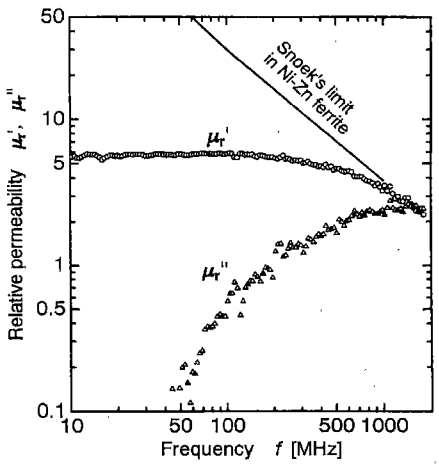

Fig. 5. Complex relative permeability of composite thick film

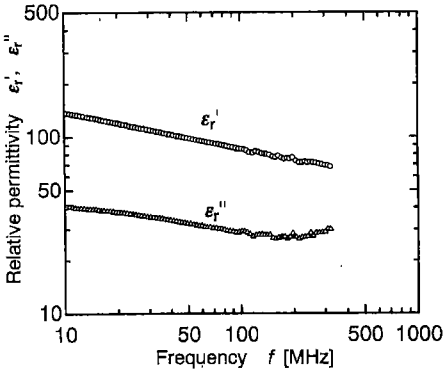

Fig. 6. Complex relative permittivity of composite thick film

3.3 Properties Fig. 4 is a typical example of the static magnetization curve of the composite thick film, which was measured by using a vibrating sample magnetometer (VSM). The saturation magnetization was about 2.6 kG, and coercive force was about 52 Oe. The volume ratio of the ferrite particle in the composite film, which was measured for ten samples, was estimated to be about 51-60% from the saturation magnetization measurement.

Fig. 5 shows the complex relative permeability of the composite film. The real part of the complex relative permeability was about 6, and the cut off frequency was about 600 MHz. For a comparison, Snoek's limit line for the bulk Ni-Zn ferrite is shown in Fig. 5. The cut-off frequency of the permeability measured for the Mn-Zn ferrite/polyimide composite film exhibited the same tendency as the Snoek's limit line for the Ni-Zn ferrite. Therefore, the composite film had the nearly the same high frequency characteristic as the bulk Ni-Zn ferrite.

The complex relative permittivity of the composite film is indicated in Fig. 6. The composite film had a relative permittivity of over several tens, which was much greater than that of the Ni-Zn ferrite. The high permittivity of the composite film was due to a very large capacitance of the grain boundary in the polycrystalline Mn-Zn ferrite particle [6].

Although not shown here, the composite film exhibited a dc conductivity of 10^{-3} S/m [5], which was 100 times higher than that of Ni-Zn ferrite. This was due to the point contact between neighboring high conductivity Mn-Zn ferrite particles [5].

4. Fabrication of Common-Mode Filter

A possibility of the application of composite material to the common-mode filter was investigated. The device fabricated here was not necessarily based on the optimum design. The photograph of the fabricated device is shown in Fig. 7. Table 1 shows the typical specifications of the fabricated device. As shown in Figs. 1

Fig. 7. Fabricated device

Table 1. Typical specifications of fabricated device

Device size	3.75 mm × 12.50 mm × 0.50 mm
Substrate	0.3 mm thick aluminum plate
Inner conductor lines	Sputtered aluminum film Thickness t_c: 3μm Width w_c: 50 μm Length l: 12.5 mm Spacing s: 40 μm
Top ground plane	Silver paste
Composite material	Mn-Zn ferrite/Polyimide hybrid Ferrite volume fraction : 51−60% Permeablity μ': 6 @100MHz Permittivity ε': 100 @100MHz Thickness t_f: 80 μm
Inner Polyimide	Spun on and cured polyimide Thickness t_p: 3 μm Permittivity ε_p': 3.5

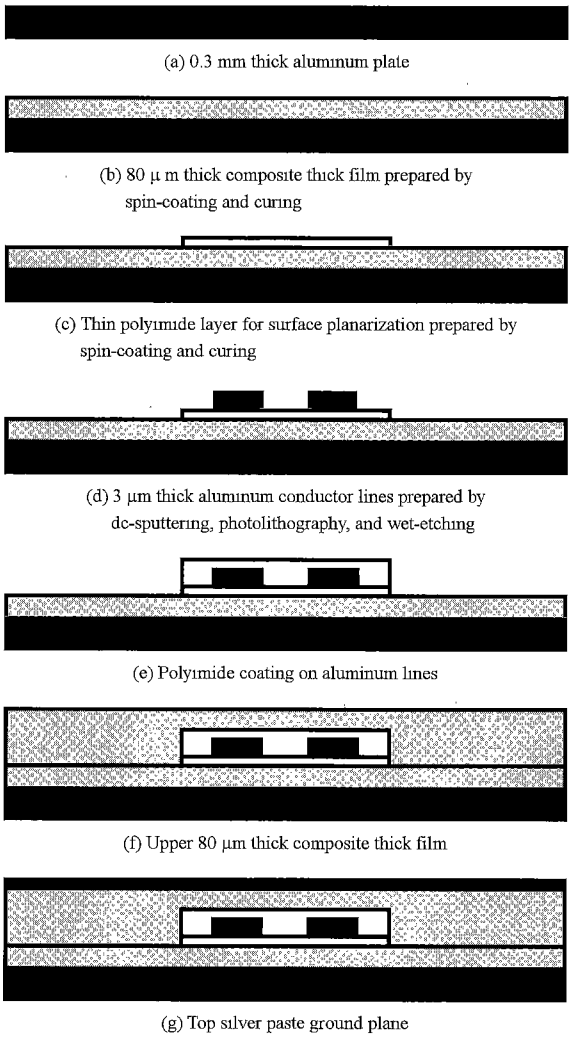

Fig. 8. Fabrication sequence of common-mode noise filter

and 7, since the fabricated device had a pair of aluminum straight conductor lines with a length of 12.5 mm; the device length was relatively long. For the miniaturization of the device, the meander line structure will be useful.

The fabrication sequence of the device is shown in Fig.8.

4.1 Lower Composite Film and Conductor Lines The lower 80μm thick composite film was fabricated on a 0.3 mm thick aluminum substrate. To smooth the surface of the composite film, the mechanical polishing was done. The 3μm thick polyimide film was fabricated on the top surface of the lower composite film. A pair of 3μm thick aluminum conductor lines was fabricated using the sputter-deposition and photolithography technique. The conductor line width was 50μm, and the spacing between the conductor lines was 40μm, respectively.

4.2 Upper Composite Film and Top Ground Plane

The 3μm thick polyimide film was fabricated on the aluminum conductor lines, and the upper 80μm thick composite film was fabricated. Finally, the top silver paste ground plane was fabricated on the top surface of the upper composite film.

4.3 Estimations of C_{11}, G_{11}, C_{12} and G_{12} C_{12} and G_{12} in Fig. 2 are due to the 40 μm wide spacing between 3μm thick aluminum conductor lines. Fig. 9(a) shows a model for C_{12} and G_{12}. The spacing was filled with the polyimide. Hence, C_{12} and G_{12} are written as follows,

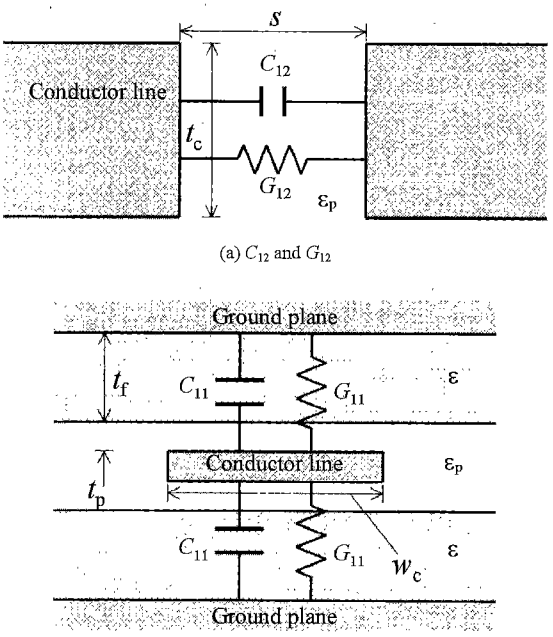

(a) C_{12} and G_{12}

(b) C_{11} and G_{11}

Fig. 9. Models for C_{12}, G_{12}, C_{11} and G_{11}

$$C_{12} = \varepsilon_p' t_c / s, \quad G_{12} = \omega \varepsilon_p'' t_c / s \quad \cdots\cdots (7)$$

where t_c is the thickness of the aluminum line, s is the spacing between two aluminum lines, ε_p' and ε_p'' are the real part and imaginary part of the complex permittivity of the polyimide in the spacing,

$$\varepsilon_p = \varepsilon_p' - j\varepsilon_p'' \quad \cdots\cdots (8)$$

The dielectric loss tangent of the polyimide, defined as $\varepsilon_p''/\varepsilon_p'$, was below 10^{-2}. Hence, ε_p'' was much smaller than ε_p'.

On the other hand, the distributed capacitance C_{11} and conductance G_{11} between the inner aluminum line and the ground plane are due the composite film layer and polyimide layer. A model for C_{11} and G_{11} is shown in Fig. 9(b). C_{11} and G_{11} are written as follows,

$$C_{11} = \varepsilon_{eff}' w_c / (t_f + t_p), \quad G_{12} = \omega \varepsilon_{eff}'' w_c / (t_f + t_p) \quad \cdots\cdots (9)$$

where w_c is the width of the aluminum line, t_f is the thickness of the ferrite/polyimide composite layer, t_p are the thickness of the polyimide layer, ε_{eff}' and ε_{eff}'' are the real part and imaginary part of the complex effective permittivity of the composite material/polyimide layer, respectively. The complex effective permittivity ε_{eff} is written as follows,

$$\varepsilon_{eff} = \frac{\varepsilon \varepsilon_p (t_f + t_p)}{\varepsilon_p t_f + \varepsilon t_p} \quad \cdots\cdots (10)$$

ε_p is the complex permittivity of the polyimide, which is indicated in Eq.(8). ε is the complex permittivity of the composite material (Fig. 6), and as follows,

$$\varepsilon = \varepsilon' - j\varepsilon'' \quad \cdots\cdots (11)$$

Table 2 shows the estimated capacitance ratio C_{11}/C_{12} and conductance ratio G_{11}/G_{12} for the fabricated device. These values were estimated from the material properties and device parameters. From the estimated C_{11}/C_{12} and G_{11}/G_{12}, the assumptions

Table 2. Estimated C_{11}/C_{12} and G_{11}/G_{12} for the fabricated device

Frequency (MHz)	10	20	30	50	70	100	200	300
C_{11}/C_{12}	136	128	123	118	112	105	98	98
G_{11}/G_{12}	15	18	19	22	24	27	30	30

($G_{11}>>G_{12}$, $C_{11}>>C_{12}$) described in Section 2.2 and the approximations of Eqs.(5), (6) were satisfied enough.

5. Experimental Method of Signal Transmission Characteristics of Common-Mode Filter

5.1 Transmission Characteristics To estimate the transmission characteristics such as characteristic impedance Z_c and propagation constant γ, the reflective coefficient S_{11} and transmission coefficient S_{21} in the scattering matrix [S] were measured using a network analyzer (HP8753D).

By using S_{11} and S_{21}, the characteristic impedance Z_c of the device is written as follows [7];

$$Z_c = 50\left\{\frac{1+2S_{11}+S_{11}^2-S_{21}^2}{1-2S_{11}+S_{11}^2-S_{21}^2}\right\}^{1/2} \quad \cdots\cdots (12)$$

The decay constant α can be written by using scattering parameters S_{11} and S_{21} [7];

$$\alpha = \frac{ln\left[A^2+B^2\right]}{4l} \quad \cdots\cdots (13)$$

where l is the conductor line length, A and B are as follows;

$$A+jB = \frac{50\left(1-S_{11}^2+S_{21}^2\right)+Z_c\left(1-2S_{11}+S_{11}^2-S_{21}^2\right)}{50\left(1-S_{11}^2+S_{21}^2\right)-Z_c\left(1-2S_{11}+S_{11}^2-S_{21}^2\right)} \quad \cdots\cdots (14)$$

The phase constant β, which is the imaginary part of the propagation constant γ, can be written by following equation [7];

$$\beta = \frac{\tan^{-1}\left[B/A\right]}{2l} \quad \cdots\cdots (15)$$

When the scattering parameters S_{11} and S_{21} were measured for the balanced-mode and common-mode conditions, Z_c and γ were estimated for both conditions.

5.2 Signal Transmission Experiments for Balanced-Mode and Unbalanced-Mode Rectangular Signals To estimate the transmission characteristics for the balanced-mode signal and unbalanced common-mode signal, a rectangular waveform signal was applied to the device using a pulse generator (HP8133A), and the frequency spectra of the input and output signals of the device were measured.

The experimental set-up is shown in Fig. 10. The input and output signals of the device under test (DUT) were measured using a sampling oscilloscope with an EO (Electro-optical) probe (Ando Electric Co. ; AQ7700). The repetitive frequency of the rectangular waveform signal was 200 MHz.

6. Experimental Results and Discussion

6.1 Transmission Characteristics Fig. 11 shows the transmission characteristics, Z_c, α and β measured for the fabricated filter, these parameters were measured in both conditions for the balanced-mode and common-mode signal. In the figure, the subscript "c" means the common-mode signal condition, the subscript "b" means the balanced-mode signal

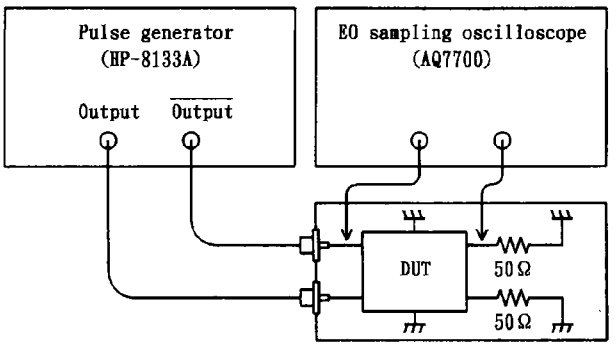

(a) For balanced-mode signal

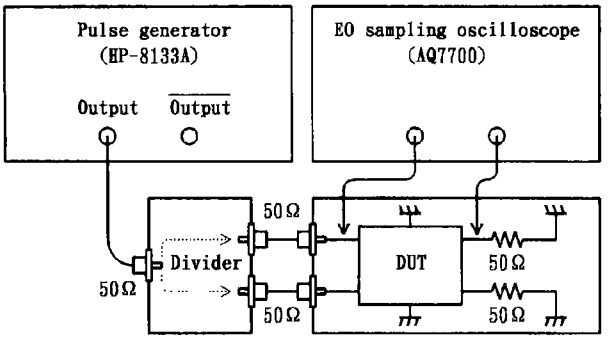

(b) For unbalanced common-mode signal

Fig. 10. Experimental set-up of rectangular waveform signal transmission

condition.

The balanced-mode characteristic impedance Z_{cb} was estimated to be about 37-72Ω, which was nearly close to 50Ω. On the other hand, the unbalanced common-mode characteristic impedance Z_{cc} was only two times larger than Z_{cb}, which was owing to the weak magnetic coupling between the inner two aluminum lines. Although not shown in detail here, the magnetic coupling coefficient k was estimated to be about 0.44 even at 100 MHz.

The decay constant α_c was larger than α_b, and the difference between α_c and α_b became large with increasing frequency. The phase constant β_c was also larger than β_b, the difference between β_c and β_b became large at high frequencies over 1 GHz. The large α_c for the unbalanced common-mode signal was due to the positive magnetic coupling between the embedded two conductor lines, and was dependent on the high frequency loss of the composite film. Since the fabricated filter had the weak magnetic coupling between the inner aluminum lines, the decay constant α_b for the balanced-mode was not negligibly small. The reason for the weak magnetic coupling may be not only due to the large spacing of 40 μm between two aluminum lines, but also due to the low relative permeability (below 6) of the composite film. In order to increase the relative permeability, it is desired to obtain the large volume fraction of the ferrite for the composite film. However, it is not so easy to fabricate the ferrite rich composite film by using the spin coating, because of the high viscosity mixture slurry with a high content ferrite particle. Therefore, a screen-printing method will be useful for obtaining the ferrite rich composite film.

The common-mode noise filter for the balanced-mode signal

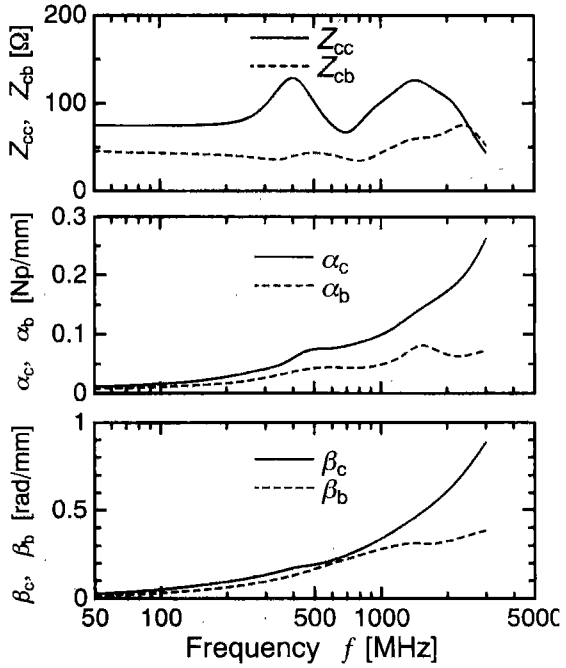

Fig. 11. Characteristic impedance Z_{cc}, Z_{cb}, decay constant α_c, α_b, phase constant β_c, β_b, estimated for the fabricated device. The subscript "c" means the common-mode condition, and "b" means the balanced-mode condition

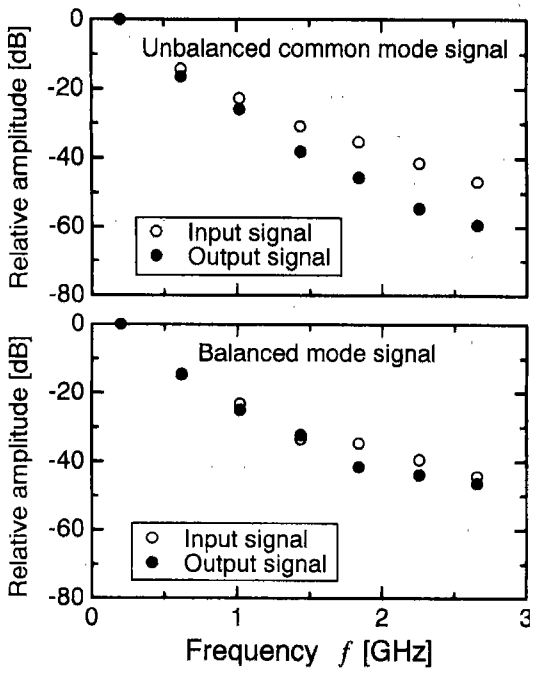

Fig. 12. Frequency spectra of input and output signal measured when the 200MHz rectangular waveform signal was applied to the fabricated device. The upper figure is for the unbalanced-mode signal, the lower figure is for the balanced-mode signal

interface should have large α_c and small α_b. In the fabricated device, both the common-mode suppression and balanced-mode transmission were obtained only at high frequencies in the GHz band, because the losses became large at high frequencies. It is currently unknown that either magnetic loss or dielectric loss is dominant.

6.2 Experimental Results of 200MHz Rectangular Waveform Signal Transmission A 200 MHz rectangular waveform signal was applied to the input terminals of the device, and the 50Ω termination resistances were connected to the output terminals. Fig. 12 shows the frequency-spectra of the input signal and output signal of the device. The result for the unbalanced-mode signal was shown in the upper figure, the result for the balanced-mode signal was shown in the lower figure, respectively.

The unbalanced signal frequency spectrum shows that the signal-decays were over 10dB at high frequencies over 1GHz. This was due to the large decay constant α_c. The balanced- mode signal-decays were small even in the high frequencies over 1GHz except some data.

The 200 MHz rectangular waveform signal includes the higher frequency components. Therefore, the measured results show that the fabricated device has the signal suppression with over 10 dB for the unbalanced common-mode signal in the GHz band. In the near future, the advanced high-speed balanced digital signal interface will be developed, which will operate at Gbps data transfer rate. For real application of the device to such advanced system, it is desired that the larger common-mode suppression and smaller decay for the balanced-mode signal will be required.

7. Conclusion

Mn-Zn ferrite particle/polyimide composite thick film was fabricated and applied to the common-mode noise filter. The fabricated filter exhibited the signal suppression with over 10 dB for the unbalanced common-mode signal in the GHz band. For the balanced-mode signal, the device exhibited the small decay at the same frequency band.

The authors consider that the device fabricated here is superior to the conventional dielectric coupled transmission-line filter, because the newly fabricated device has the wide band common-mode suppression. However, the common-mode noise rejection is not so enough. This is mainly due to the weak magnetic coupling between the inner two aluminum lines. In order to improve it, the large volume fraction of the ferrite will be required for the composite film, and the narrow spacing between the two conductor lines will also be required for the device.

Acknowledgement

This work was supported by the grant of the Ministry of Education, Culture, Sports, Science and Technology, Japan (#.14550322).

(Manuscript received Aug. 30, 2002, revised June 19, 2003)

References

(1) T. Wright : "USB: New technology holds a lot of promise for computer users", *Dayton Dairy News*, Vol.8 (1998)

(2) H Kitayama : Architecture of IEEE 1394 Interface, Vol 7, pp.58-68, Interface (CQ Publishing Co) (1999) (in Japanese)

(3) F Tsuda, Y. Kaizaki, S. Shinohara, and R Sato : "A study on response of common mode filter with a multilayer structure", The Papers of Technical Meeting, IEEJ, MAG-98-257 (1998)

(4) T. Sato, S. Ikeda, Y. Hara, K. Yamasawa, and T. Sakuma : "A new multilayered common-mode filter on Ni-Zn ferrite substrate", *IEEE Trans. Magn.*, Vol. 37, No.4, pp.2900-2902 (2001)
(5) T. Kokai, T. Sato, K. Yamasawa, H. Karasawa, and T. Sakuma : "Fabrication of a Mn-Zn Ferrite Particle/Polyimide Composite Thick Film", *J. Mag. Soc. Japan*, Vol.26, pp.484-489 (2002)
(6) J. Smit and H. P. Wijn : Ferrites, pp.236-242, Philips Technical Library (1959)
(7) Y. Fujishiro : "Evaluation for electronic components by *S* parameters", *Product Hotline Magazine, TDK*, Vol.33, pp. 27-33 (1999)

Toshiro Sato (Member) received the B. E., M. E. and Ph. D degrees in Electrical Engineering from Chiba University, Chiba, Japan, in 1982, 1984 and 1989, respectively. In 1989, he joined the TOSHIBA R&D Center. He is now an associate professor, Shinshu University, Nagano, Japan. He has been engaged in the research and development of the high frequency magnetic thin film devices.

Takahiro Kokai (Non-member) received the B. E. and M. E. degrees in Electrical and Electronic Engineering from Shinshu University, Nagano, Japan, in 2000 and 2002. In 2002, he joined the Nagano Japan Radio Corporation, Nagano, Japan. He has been engaged in the development of high frequency devices

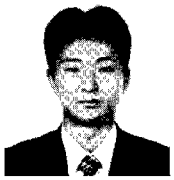

Masashi Moroishi (Non-member) is currently with the M. E. cource of the graduate school of the Science and Technology, Shinshu University, Nagano, Japan. He has been engaged in the research and development of the common mode filter device.

Kiyohito Yamasawa (Member) received the B. E., M. E. and D.E. degrees in Electrical Engineering from Tohoku University, Sendai, Japan, in 1966, 1968 and 1979, respectively. He is currently a professor, Shinshu University, Nagano, Japan. His research interests include the magnetic device, magnetic actuator, micro switching power supplies.

Toshiyuki Sakuma (Non-member) received the B. E., M. E. and D. E. degrees from Shinshu University, Nagano, Japan, in 1981, 1983, and 1999, respectively. He joined the NEC Corporation in 1983, where he was involved with the application of ferroelectric thin films for DRAM cell-capacitors. In 1999, he joined KOA Corporation.

Hiroki Karasawa (Non-member) received the B. E. and M. E degrees in mechanical engineering from Nihon University, Fukushima, Japan, in 1995, 1998 respectively. In 1998, he joined the KOA Corporation. He is currently developing thin-film fuse in the Product Development Center.

Koichi Hirasawa (Member) received the B. E. and M. E. degrees from Tokyo University of Science, Tokyo, Japan, in 1990. He joined the Nagano NEC Ltd. in 1990. In 1999, he joined the KOA Corporation.